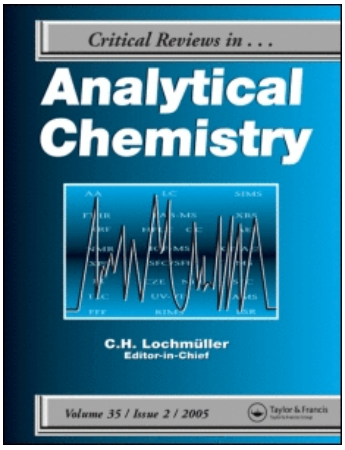

Critical Reviews in Analytical Chemistry
Publication details, including instructions for authors and subscription information:
http://www.informaworld.com/smpp/title~content=t713400837

Square-Wave Polarography and Related Techniques

Gary D. Christian; Donald Rosenthal

To cite this Article Christian, Gary D. and Rosenthal, Donald(1975) 'Square-Wave Polarography and Related Techniques', Critical Reviews in Analytical Chemistry, 5: 2, 201 — 223
To link to this Article: DOI: 10.1080/10408347508542684
URL: http://dx.doi.org/10.1080/10408347508542684

SQUARE-WAVE POLAROGRAPHY AND RELATED TECHNIQUES

Authors: Peter E. Sturrock
Georgia Institute of Technology
Atlanta, Georgia

Richard J. Carter
Medical University of South Carolina
Charleston, South Carolina

Referee: Louis Ramaley
Dalhousie University
Halifax, Nova Scotia, Canada

TABLE OF CONTENTS

I. INTRODUCTION

Conventional polarography (called DC polarography below) has found wide application as an analytical tool because it is applicable to both inorganic and organic systems, exhibits a linear response over several orders of magnitude of concentration, and gives information about oxidation state and degree of complexation. However, DC polarography is not satisfactory at concentrations below about $10^{-5}M$ and cannot analyze for species at that level in the presence of a high concentration of a more readily reducible species (e.g., Cd^{+2} in the presence of Pb^{+2}). A number of variations of polarography have been developed in attempts to improve performance. One of the most promising of these variations is square-wave polarography.

Recognizing that there are several conflicting definitions, square-wave polarography, as used in this review, encompasses a group of related techniques in which one or more rectangular pulses of small amplitude (<100 mv) are applied to a polarized electrode. These pulses are superimposed on a base potential that is stepped or scanned at a specified rate, and the cell current is measured at specified times during the process. The cell may be either of two- or three-electrode configuration, and the working electrode may be either a dropping-mercury electrode (D.M.E.) or an electrode of fixed surface area. Thus, in addition to that technique first known as square-wave polarography, this review includes techniques more commonly known as differential-pulse polarography, differential-pulse voltammetry, square-wave voltammetry, and their applications to anodic stripping analysis. These techniques are all related in that they separate faradaic and capacitance currents by time delay.

II. REVIEW OF TECHNIQUES

Square-wave polarography was first reported by Barker and Jenkins.[1] Their instrument used vacuum-tube circuits, relay switching, and a two-electrode cell. A 225-Hz square wave of variable magnitude was used. The authors described operation with both a D.M.E. and stripping analysis with a single mercury drop. In subsequent papers, Barker and co-workers developed the theory and instrumentation[2-6] while Milner and co-workers reported on applications.[7-10] The square-wave polarogram resembles the derivative of a DC polarogram and offers significant improvement in sensitivity, in resolution between successive peaks, and in ability to measure a small wave following a large wave.

Sensitivity was reported as $2 \times 10^{-7}M$ for reversible systems. Barker, Faircloth and Gardner[5] reported an improved instrument with a sensitivity of $4 \times 10^{-8}M$ for reversible systems and of $1 \times 10^{-6}M$ for irreversible systems with a D.M.E., and about 100 times improved sensitivity for the stripping technique. The sensitivity with the D.M.E. was limited by "noise" originating in the capillary. This capillary noise was thought to result from the long time constant for the decay of the capacitance current associated with the solution that crept up the inside of the capillary and adjacent to the mercury thread. This capillary noise changed in an erratic manner and produced sharp spikes on the recorded polarogram, even when supporting electrolyte concentrations of $0.2M$ or greater were used.

Barker and Gardner[11] concluded that the problem of the capillary noise could be avoided by using a lower-frequency square wave (10 Hz) and thereby increasing the time between pulse application and sampling to about 40 msec from the 2.2 msec used in their earlier instruments. However, this resulted in fewer square waves per drop and created design problems in the instrumentation, which the authors did not describe. To circumvent these design problems, they elected to apply only one 40-msec pulse per drop and to sample the current during the last half of the pulse time. Thus the current was sampled for 20 msec after the 20-msec delay following pulse application. It should be pointed out here that 20 msec is exactly one cycle time of the 50-Hz line frequency used in England. Since the wave noise signal originating from the power lines is algebraically added to the desired signal, some reduction in noise interference is obtained by averaging the signal over one or more complete cycle times of the noise. This averaging during the sampling process is necessary, since the pulse repetition rate was the same as the drop time (>2 sec) and RC filtering is quite difficult at this low frequency. Barker and Gardner[11] reported detection limits of $1 \times 10^{-8}M$ and $5 \times 10^{-8}M$ respectively for reversible and irreversible processes in favorable cases. In addition, it was possible to work at lower concentrations of supporting electrolyte. The increased

sensitivity of pulse polarography for irreversible processes is probably due in large part to the use of lower concentrations of supporting electrolyte. This relationship was reported by Sturm and Ressel.[12]

Barker and Gardner[11] referred to the polarograms obtained by this pulse-polarographic technique as derivative polarograms, since they resembled the shape of the derivative of the DC polarogram. This technique is now commonly known as differential-pulse polarography. Barker and Gardner[11] also reported another form of pulse polarography, in which the polarogram looks like a DC polarogram. This technique is now called normal-pulse polarography.[15] In this technique, each pulse is increased in magnitude of voltage over the previous one and the potential returns to the same rest potential between each pulse. This form of pulse polarography has advantages when slow adsorption occurs in some of the potential regions. However, it is generally less sensitive than differential-pulse polarography.

Some pulse polarographs have a third mode of operation, in which the differences in currents between successive pulses of a normal-pulse polarogram are recorded. This technique is known as derivative-pulse polarography, but it is distinctly different from differential-pulse polarography.

Ramaley and Krause[13] devised a method which they called square-wave voltammetry. In this technique the potential change on pulse application is larger than the subsequent change on pulse relaxation, so that the excitation wave-form looks as if a square wave were superimposed on a synchronized stair step signal. The technique used a stationary electrode and featured the relatively fast sweep rate of 20 mv/sec as contrasted to the 1 mv/sec typical of pulse polarography. These workers reported a detection limit of $2.5 \times 10^{-8} M$ for reversible systems with a three-electron transfer.

All of the techniques described above have been applied to anodic stripping and show significantly higher sensitivities than the linear-sweep voltammetry commonly used in stripping analysis.

III. THEORETICAL CONSIDERATIONS

In DC polarography there are two important sources of current: the faradaic current, which is proportional to the concentration of the depolarizer when the process is diffusion-controlled, and the capacitance current required to charge the electrode to the desired potential as the drop area increases. When the potential is suddenly stepped by the application of a pulse, several other currents must be considered.

First, there is the pulse faradaic current, which is again proportional to the concentration of depolarizer and results from the change in the heterogeneous rate constant as the potential is stepped. This is the current that should be measured by a square-wave polarograph. Second, there is the pulse capacitance current required to charge the electrode double layer to the new potential. Third, there is a change in the DC capacitance current, because the expanding drop is at a different potential than prior to pulse application. This change in the DC capacitance current is included in the current recorded by most square-wave and pulse polarographs and was recently discussed by Christie and Osteryoung.[14] For optimal sensitivity, a square-wave polarograph must be designed so that the ratio of the pulse faradaic current to the sum of all other currents is maximized.

A. Pulse Faradaic Current

The theoretical equation for the pulse faradaic current in a square-wave experiment was derived by Barker and co-workers[3,5] and is given by

$$i = \frac{n^2 F^2}{RT} C_o \Delta E \frac{P}{(1+P)^2} \left(\frac{D_o}{\pi\tau}\right)^{1/2} \sum_{m=0}^{\infty} (-1)^m \frac{1}{(m+\beta)^{1/2}} \text{ amp cm}^{-2} \qquad (1)$$

In this equation ΔE is the magnitude, τ is the half-cycle time of the square wave, F is the Faraday, R is the gas constant, T is the absolute temperature, C is the concentration, D is the diffusion coefficient, and n is the number of electrons in the half-reaction equation. β is the fraction of the half-cycle time at which the current is measured, and m (see Figure 1, a and b; $\beta = t/\tau$) is a positive integer. The factor P is equal to $\exp(E - E_{1/2})nF/RT$. The other symbols have their usual significance. The equation is only valid for diffusion-controlled conditions and when ΔE is $\ll RT/nF$. If only the first half-cycle is considered, as is common in pulse polarography, Equation 1 reduces to

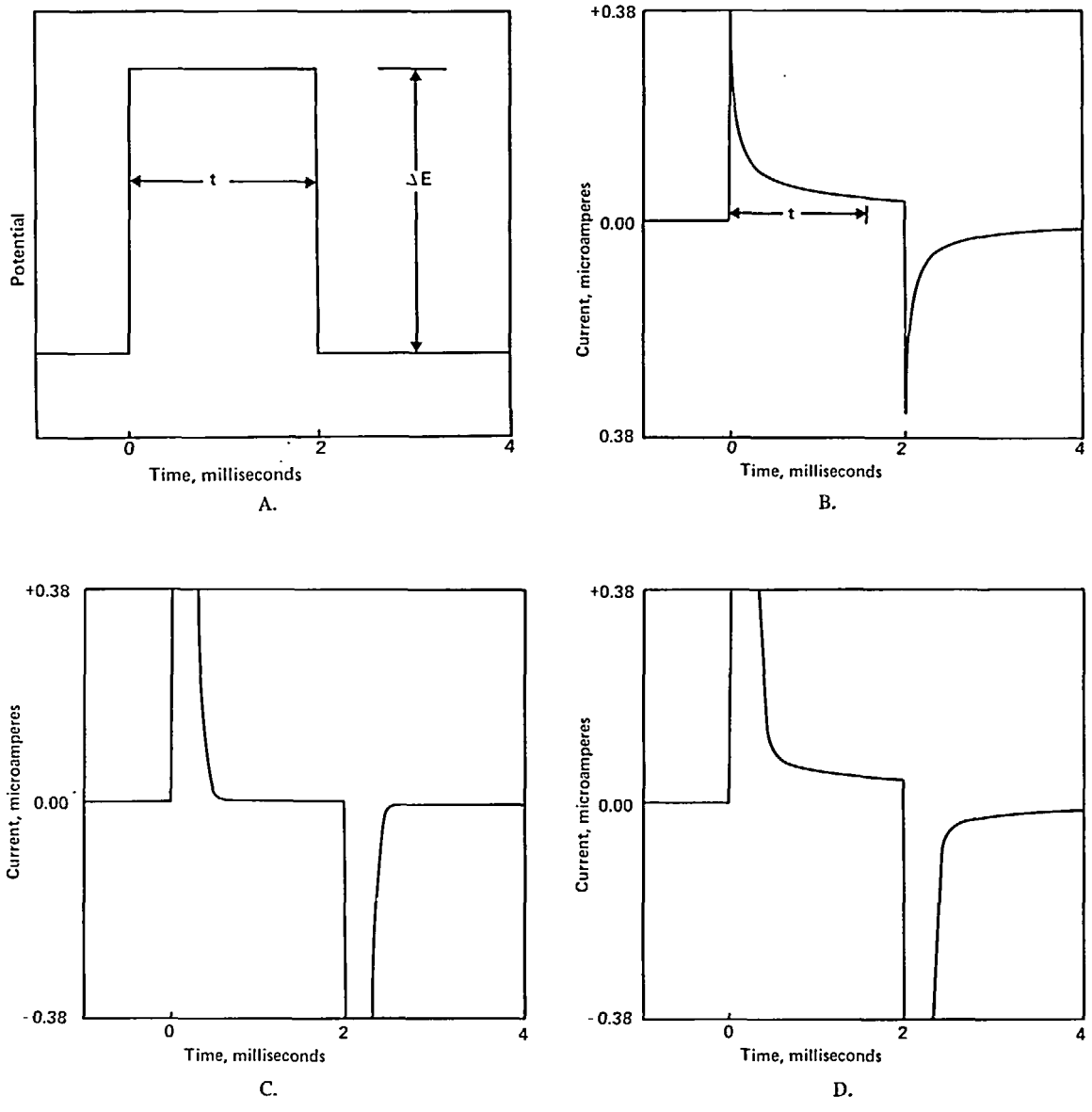

FIGURE 1. Pulse application and current responses. A. Potential pulse. B. Pulse faradaic current, $1 \times 10^{-7} M$ Pb^{2+}, A = 0.025 cm^2, ΔE = 25 mV. C. Pulse capacitance current, c = 20 $\mu F/cm^2$, A = 0.025 cm^2, R = 100 Ω, ΔE = 25 mV. D. Total current (sum of B and C).

$$i = \frac{n^2 F^2}{RT} C_o \Delta E \frac{P}{(1+P)^2} \left(\frac{D_o}{\pi\tau\beta}\right)^{1/2} \text{amp cm}^{-2} \qquad (2)$$

The product, $\tau\beta$, can be replaced by t, the time between pulse application and current sampling.

Parry and Osteryoung[15] derived a more general equation for pulse polarography that eliminates the restrictions on pulse size inherent in Equations 1 and 2. Their equation is

$$i = nFAC_o \left[\frac{D_o}{\pi t}\right]^{1/2} \left(\frac{P_A\delta^2 - PA}{\delta + P_A\delta^2 + PA + P_A{}^2\delta}\right) \qquad (3)$$

where

$$P_A = \exp\left(\frac{E_1 + E_2}{2} - E_{1/2}\right) \frac{nF}{RT}$$

and

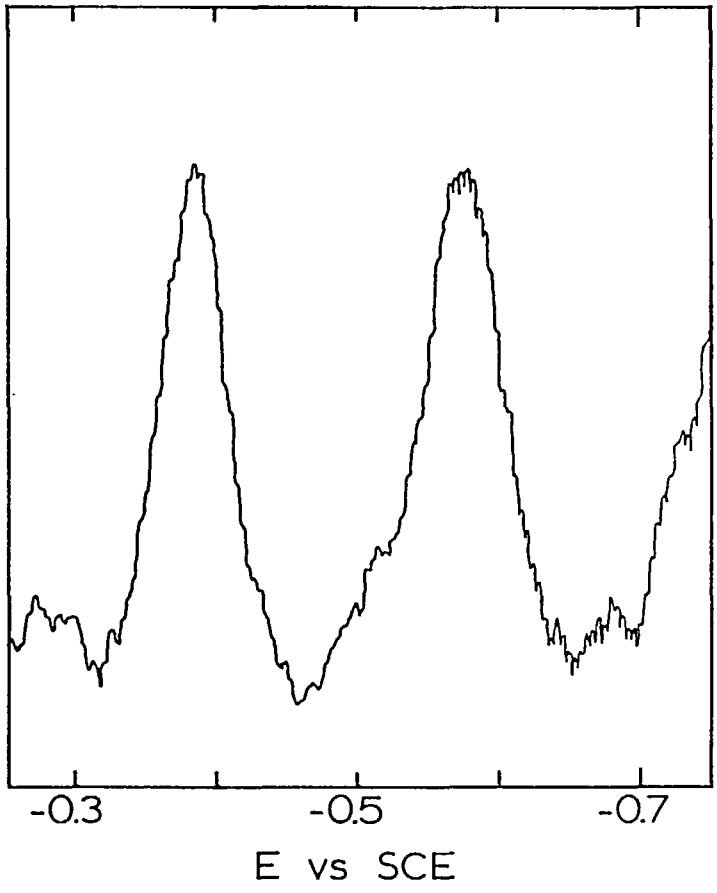

FIGURE 2. Square-wave polarogram of $5 \times 10^{-8}M$ Pb^{2+} and $5 \times 10^{-8}M$ Cd^{2+} in $0.05M$ KNO_3. Square-wave is 30 Hz and 15 mV p-p. Positive feedback is 380 Ω compensation. Sweep rate is 1 mV/sec.

$$\delta = \exp\left(\frac{(E_2 - E_1)}{2}\frac{nF}{RT}\right)$$

E_1 and E_2 are the potentials between which the potential is stepped. An analogous equation for square-wave polarography could be readily derived. By plotting pulse size versus faradaic current as calculated by Equation 3, it is seen that the increase in current is almost proportional to pulse size up to about a 20-mV pulse and increases at a slower rate for larger pulses.

In Equation 1, the term $P/(1 + P)^2$ determines the shape of the peaks of the polarogram. As pointed out by Barker, Faircloth and Gardner,[5] the width of the peaks at half the peak current should be 90.4/n mV. This is the same as in AC polarography and derivative DC polarography. If ΔE is large enough so that Equation 1 is not valid, the peak widths can be deduced from Equation 3. Barker, Faircloth and Gardner[5] also report equations analogous to Equation 1 for "slightly irreversible" and "highly irreversible" reactions. The reader is referred to the original literature for details. Qualitatively, the peaks decrease in height and increase in width as irreversibility increases.

Figure 2 illustrates a square-wave polarogram of lead and cadmium. The peak potentials of -0.39 and -0.58 V vs. SCE are equal to the half-wave potentials of these species in a DC polarogram. As predicted in Equation 1, the peak height is directly proportional to concentration and n^2.

B. Pulse Capacitance Current

The pulse capacitance current is given by

$$i_c = (\Delta E/r) \exp(-t/rc) \text{ amps} \quad (4)$$

TABLE 1

t (msec)	A (cm^2)	C ($\mu f/cm^2$)	r (ohms)	r × c × A (μsec)	i_f (amp × 10^7)	i_c (amp)	i_f/i_c
0.5	0.025	20	100	50	0.749	1.13×10^{-8}	6.63
0.5	0.025	20	200	100	0.749	8.42×10^{-7}	8.90×10^{-2}
0.5	0.025	40	100	100	0.749	1.68×10^{-6}	4.46×10^{-2}
0.5	0.050	20	100	100	1.498	1.68×10^{-6}	8.92×10^{-2}
1.0	0.025	20	100	50	0.530	5.15×10^{-13}	1.03×10^{5}
1.0	0.025	20	200	100	0.530	5.67×10^{-9}	9.35
1.0	0.025	40	100	100	0.530	1.13×10^{-8}	4.69
1.0	0.050	20	100	100	1.059	1.13×10^{-8}	9.37
1.5	0.025	20	100	50	0.432	2.34×10^{-17}	1.85×10^{9}
1.5	0.025	20	200	100	0.432	3.82×10^{-11}	1.13×10^{3}
1.5	0.025	40	100	100	0.432	7.65×10^{-11}	5.65×10^{2}
1.5	0.050	20	100	100	0.865	7.65×10^{-11}	1.13×10^{3}
2.0	0.025	20	100	50	0.375	1.06×10^{-21}	3.54×10^{13}
2.0	0.025	20	200	100	0.375	2.58×10^{-13}	1.45×10^{5}
2.0	0.025	40	100	100	0.375	5.15×10^{-13}	7.28×10^{4}
2.0	0.050	20	100	100	0.749	5.15×10^{-13}	1.45×10^{5}

where t is the time in seconds after pulse application, c is the capacitance of the electrode double layer in farads, and r is the composite resistance, in ohms, of the mercury thread, the solution, and the output stages of the control amplifier. Thus, decreasing the rc product decreased i_c for times greater than 0 without decreasing the faradaic current. Barker[6] kept the supporting electrolyte concentration between 0.2 and 1*M* to minimize the solution resistance and maximize the ratio of the pulse faradaic to pulse capacitance current. With the use of the three-electrode cell configuration, and especially with modern solid-state potentiostats, the effective cell resistance is greatly reduced, even in solutions of much more dilute supporting electrolyte. This may be the reason why neither the present authors nor Buchanan[16] have observed the capillary noise that caused Barker[11] to go to the long delay times and finally to pulse polarography.

Since the pulse capacitance current decays more rapidly than the pulse faradaic current, the ratio of the two currents continues to increase the longer the current sampling is delayed after pulse application (see Figure 1). However, once this ratio is large enough, there is no point in further delaying the sampling, as the ratio of pulse faradaic current to electronic noise decreases with increased delay. Thus, there should be some optimal time delay before sampling that depends on the double-layer capacitance, effective resistance, electrode area, depolarizer concentration, and electronic noise level. Table 1 gives some comparisons for the peak pulse faradaic current and pulse capacitance current for a $1 \times 10^{-7}M$ solution of a divalent metal ion with a diffusion coefficient of 1×10^{-5} cm^2/sec and a potential step of 25 mV.

In Table 1, the pronounced effect of cell-potentiostat rise time (= resistance × capacitance/unit area × area; rcA) is clearly evident. With present technology, rise times of less than 50 μsec are readily obtainable, even with 0.01*M* supporting electrolyte, if a positive-feedback loop is used in the potentiostat. However, even with rise times of 100 μsec, the ratio of peak pulse faradaic current (simple pulse faradaic current) to pulse capacitance current is on the order of 10^5 after a delay of only 2 msec. Even a delay of 1 msec will give a ratio of approximately 5 with this rise time. Thus, it hardly seems necessary to delay more than 1 msec before sampling, unless a very dilute supporting electrolyte or a very poor potentiostat is used. If the sampling is done after a 20- or 40-msec delay, the faradaic current would be 22 or 16% respectively of that at 1 msec.

Instead of measuring the current after application of the pulse, as was done for the data in Table 1, it is quite possible to measure the difference between that current and the current measured after the potential is stepped back to the original value (difference pulse faradaic current).

The capacitance current resulting from this pulse relaxation will be opposite in sign and almost equal in magnitude from that of the pulse application, provided the pulse time is many times longer than the cell-potentiostat rise time. On the other hand, the faradaic current associated with the pulse relaxation will be opposite in sign, but smaller in magnitude (see Figure 1, b and c). Thus, the difference pulse faradaic current will be larger than the simple pulse faradaic current, but the ratio of faradaic to capacitance currents will be smaller. For example, the difference values corresponding to the last line of Table 1 would be $\Delta i_F = 1.098 \times 10^{-7}$ amps, $\Delta i_c = 1.03 \times 10^{-12}$ amps, and the ratio = 1.06×10^5.

If multiple square waves are applied to the electrode, the faradaic current for each successive pulse application will decrease and that for each successive relaxation will increase if the electrode reaction can be reversed. The difference faradaic current for each successive cycle of the square wave will decrease rapidly at first and then approach a constant value. For example, using a 225-Hz square wave and measuring the current at the end of each half-cycle as Barker[1] did, the difference currents at the end of the 5th, 10th, 20th and 50th cycles would be 94.2, 93.8, 93.6, and 93.6% respectively of that of the first cycle. Clearly, a small loss in theoretical sensitivity results. However, the multiple current values obtained from the successive square waves are much more amenable to averaging and noise filtering than is the single value per drop obtained in pulse polarography. This is the primary advantage of square-wave polarography. In addition, a faster potential sweep is feasible, since more information is obtained per drop. Also, filters with faster time constants can be used, thus reducing distortion of the recorded peaks.

Liddle[17] made an experimental investigation of the decay of faradaic current after the application of a continuous square wave. He performed double-step chronocoulometric experiments (i.e., application of a rectangular potential pulse and integration of cell current over the pulse cycle) on a D.M.E. and compared the results of the application of one pulse with those obtained with a continuous square wave. The drop time was 4.4 sec, and a delay of 4.2 sec was used before applying a single pulse. With a solution $1 \times 10^{-3} M$ in $Cd(NO_3)_2$ and $1M$ in KNO_3, the difference between the change, Q, at the end of the first half-cycle time and Q at the end of the second half-cycle time was 0.15 μc for a half-cycle time of 0.47 msec, and 1.14 μC for a half-cycle time of 15 msec. A correction for charging the double layer is included in these values. When a continuous square wave was applied throughout the life of the drop and a single cycle at 4.2 sec into the drop life was examined, the values found were 0.14 μC and 1.14 μC respectively for the two half-cycle times.

This experiment was repeated with a solution of $1 \times 10^{-3} M$ in $Zn(NO_3)_2$ instead of in $Cd(NO_3)_2$. For a single cycle, the Q values were 5.6×10^{-3} and 0.17 μC respectively for the two half-cycle times. For the continuous square wave, the values were 7.3×10^{-3} and 0.18 μC.

It was concluded from these data that, within the experimental accuracy, there was no difference between the Q values when a single pulse and when a continuous square wave was applied. Another interesting factor is evident from these data. The relative increase in Q values with the longer half-cycle time is greater for the irreversible Zn process than for the reversible Cd process. This results because the faradaic current for the reversible process decays at a faster rate than that for the irreversible process, which is limited by the kinetics of the electron transfer reaction.

C. DC Capacitance Current

Recently, Christie and Osteryoung[14] examined the direct-current effects in pulse polarography at the D.M.E. In their calculations, the usual DC capacitance current was combined with the change in that current resulting from the change of potential with pulse application. These authors deduced that the sum of these two currents was the factor that limited the sensitivity of pulse polarography in some cases. No indication was given concerning the relative magnitudes of these two currents, but these can be calculated readily. The DC capacitance current is given by

$$i_c = (dA/dt)\, q = km^{2/3} t^{-1/3} q \qquad (5)$$

where q is the charge on the electrode and the value of k at 25°C is 0.00569. Using the data of Grahame,[18] it is possible to estimate the magnitudes of the two portions of the DC capacitance current. The charge on the electrode is estimated to be 4.705 $\mu C/cm^2$ at -0.375 V vs. S.C.E. and 2.776 $\mu C/cm^2$ at -0.425 V vs. S.C.E. for $0.1M$ KCl. With a flow rate of 2.5 mg/sec of mercury, after 2

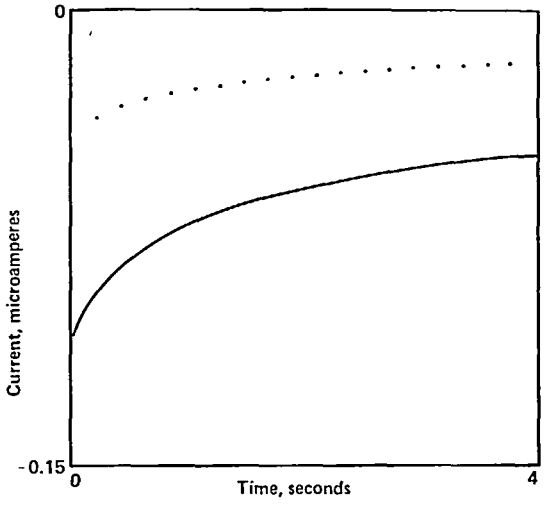

FIGURE 3. DC capacitance current of 0.1*M* KCl with 2.5 mg/sec Hg flow rate. ——= −0.375 Vvs. SCE; . . . . . = −0.425 Vvs. SCE.

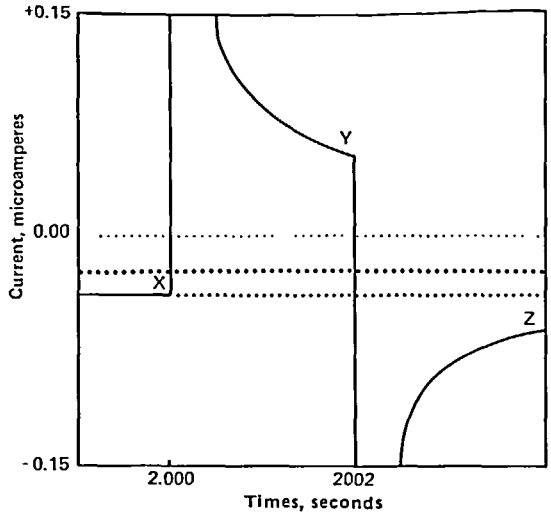

FIGURE 4. Distortion of current response by DC capacitance current. ——= total current for 1 × 10^{-7}*M* Pb^{2+} in 0.1*M* KCl; . . . . . = DC capacitance current for 0.1*M* KCl at −0.375 Vvs. SCE; • • • • • = DC capacitance current for 0.1*M* KCl at −0.425 Vvs. SCE; Hg flow rate = 2.5 mg/sec. See text for discussion.

sec of drop growth, the capacitance current would be 0.0390 and 0.0231 μA respectively at the two potentials, a change of 0.0160 μA (see Figure 3). If the electrode area continues to grow at −0.425 V, at 2.04 sec the capacitance current would be 0.0229 μA, an additional change of 0.0002 μA from that at 2 sec. If the sampling delay is shortened from the 40 msec used in this example, this second part of the change in DC capacitance would be even smaller. Thus, the important factor is the change in current resulting from the difference in electrode charge at the two potentials, and the usual capacitance current associated with the actual growth in drop area is negligible when the difference in current at the two potentials is measured (see Figure 4).

Christie and Osteryoung[14] pointed out the importance of pulse application as late as possible in the drop life where the rate of growth of the electrode area is at a minimum. It is readily shown that the ratio of pulse faradaic current to this DC capacitance current is directly proportional to the time in the drop life at which the pulse is applied. Unfortunately, the adoption of longer drop times would necessitate an even slower potential sweep, since only one data point is recorded on each drop, and thus aggravate a problem that is already one of the chief drawbacks of pulse polarography. An alternate method of improving the ratio of pulse faradaic current to DC capacitance current would be to use a shorter delay time between pulse application and current measurement, as has been discussed above (Section III B).

In their paper, Christie and Osteryoung[14] describe two types of pulse polarographs. Type 1 measures only the current at a delay time after pulse application (Figure 4, point Y) and does little to reject DC currents. Type 2 measures the difference in the current prior to pulse application and at the delay time after pulse application (Figure 4, point Y − point X), thus rejecting a substantial portion of the DC currents. However, the DC charging currents discussed above are not rejected. A third type of pulse polarograph, not described by Christie and Osteryoung, offers some improvement. If the difference between the currents at the delay time after pulse application and at the same delay time after pulse relaxation is measured (Figure 4, point Y−point Z), the DC capacitance current would be almost identical to that of the type 2 instrument, but the pulse faradaic current would be significantly larger. Almost complete rejection of the DC capacitance current should be possible by measuring the difference between point X and point Z of Figure 4.

Ramaley and Krause[13] made an interesting observation on the interrelationships of the difference pulse faradaic current, the delay time between pulse application and sampling, and the

half-cycle time of the square wave. For a constant sampling delay time, the difference pulse faradaic current increases as the half-cycle time increases. This results from the fact that, with a longer pulse, the faradaic current decays to a lower value at the end of the pulse and the faradaic current for the pulse relaxation is superimposed on a smaller background, thus giving a larger difference current. This advantage carries over with multiple square waves. For example, compare the difference currents measured with a 1-msec delay, a 1-msec half-cycle time (500 Hz), and a 10-msec half-cycle time (50 Hz). For the 500-Hz square wave, the difference current after 50 cycles is 93.6% of that for the first cycle. For the 50-Hz square wave, the difference current for the first cycle is 131% of that for 500 Hz, and after 50 cycles is 127% of the first cycle at 500 Hz and 136% of the 50th cycle at 500 Hz. Of course, this improvement must be weighed against the decreased number of measurements per drop and the concurrent impairment in averaging and filtering.

The effect of Ramaley and Krause can be combined with the enhanced current signal obtained by sampling at a shorter delay time after pulse application and relaxation. For example, consider the case of a $1 \times 10^{-8} M$ divalent depolarizer with a diffusion coefficient of 1×10^{-5} cm^2/sec, an electrode area of 0.025 cm^2, and a 10-Hz square wave of 25-mV magnitude. The faradaic current 40 msec after pulse application (type 2 instrument) is calculated to be 8.4×10^{-10} A. The difference current, measured with 1 msec delays after potential changes is calculated to be 9.9×10^{-9} A. This should result in more than a tenfold increase in sensitivity, provided the pulse capacitance current is negligible at 1 msec. In this example the ratio of pulse faradaic current to pulse capacitance current is calculated to be 7,982, assuming an effective cell resistance of 50 Ω and a differential double-layer capacitance of 39 μF/cm^2, the value for 0.1M KCl at -0.40 V vs. S.C.E.[18]

D. DC Faradaic Current

Christie and Osteryoung[14] also considered the effect of the faradaic DC polarographic current. They concluded that it decreased with decreasing concentration of depolarizer and was negligible except at very short drop times or small pulse sizes. It would be even more negligible if difference currents and shorter delays before sampling were used.

E. Stationary Electrodes

If the D.M.E. is replaced with a hanging mercury drop, thin-film mercury electrode, or other electrode of fixed area, the DC capacitance current should disappear, since that current is proportional to the rate of growth of surface area. The DC faradaic current should be less than that on the D.M.E., and the pulse capacitance current should be unchanged.

The cell-potentiostat rise time is often increased with a stationary electrode, since the resistance between the electrode and ground, or the summing point of a current-follower amplifier, is usually less than for a D.M.E. Also, if a positive-feedback loop is used in the potentiostat, it can be adjusted more precisely than when the resistance and capacitance vary with a growing electrode.

Other considerations of stationary electrodes will be discussed in Section V on applications.

F. Current Integration

The current was sampled in early instruments by gating the output of the cell-current amplifier into the input of an RC network that acted as a low-pass filter. In later instruments, sample and hold circuits have been used. Sturrock and Carter[19] reported the use of a gated integrator to measure the charge passing through the cell during selected portions of the square-wave cycle. This has the obvious advantage that a larger signal is available for processing than if a sample and hold or low-pass filter is used. In addition, the integrator circuit serves effectively to average high-frequency noise. More details of the circuitry are given in Section IV on instrumentation.

A further improvement should result if the integrated values of each square wave are summed for each drop of the D.M.E. This has not yet been done in an analog instrument, but is presently being studied by Sturrock and Hayman[19b] with a potentiostat interfaced to a laboratory minicomputer. Preliminary results look promising.

Examination of Equation 1 shows that integration of the current signal should not alter the shape of the current peaks. This has been verified by computer simulation and experimentally by Sturrock and co-workers with both analog and digital integration.

IV. INSTRUMENTATION

During the past two decades, advances in electronic components and circuits have been so rapid that most instruments described in the literature are only of historical interest. Likewise, any instrument designed today will probably become obsolete within a few years. In the author's laboratory, square-wave polarographs are constantly undergoing modification and updating to the extent that it is difficult to tell when one model is replaced with another.

Standing out from the myriad of other developments are three major steps in polarographic instrumentation: the three-electrode cell, the operational amplifier, and the use of the programmable digital minicomputer.

A. Three-electrode Cell

The early square-wave and pulse polarographs of Barker and co-workers[1-11] used the two-electrode cell configuration. In these instruments the effective resistance was the total cell resistance, and it was necessary to use high concentrations of supporting electrolyte to achieve a relatively fast rise time and reduce the pulse capacitance current to an acceptable level. The use of a three-electrode cell with a reference electrode through which no appreciable current flows allows measurement, and hence control, of electrode potential free of the major portion of the solution IR drop. A small amount of uncompensated resistance remains, which can be further reduced by the use of a positive feedback loop in the potentiostat.[20]

The use of the three-electrode cell has resulted in lower effective resistances, and therefore faster rise times for the cell-potentiostat combination. It also allows the use of lower concentrations of supporting electrolyte. As pointed out above, the use of lower concentration of supporting electrolytes decreases the problem of trace impurities in the supporting electrolyte. In addition, some irreversible processes show a marked increase in reversibility at lower concentrations of supporting electrolyte. Sturm and Ressel[12] studied this effect for the reduction of Zn^{2+} and Ni^{2+} in several supporting electrolytes. Liddle[17] determined the kinetic parameters for the Zn^{2+}/Zn amalgam electron transfer as a function of concentration of KNO_3. He concluded that the charge-transfer reaction of zinc in nitrate medium is by a consecutive-step mechanism, with the transfer between Zn^{2+} and Zn^{+} the rate-determining step at moderately high ionic strengths. As the ionic strength is lowered, mixed rate control between the two steps is observed. The reactions are first order with respect to Zn^{2+} and Zn^{0}.

The present authors have never observed the "capillary noise" reported by Barker and Jenkins[1] and believe that this may be a result of the use of the three-electrode cell. Buchanan[16] reports similar experiences, except with a capillary that was damaged by application of extreme potential. Both the present authors and Buchanan have used only capillaries supplied by the Sargent-Welch Company.

B. Square-wave Polarographs

Many articles and reviews are to be found in the literature on the theory and application of operational amplifiers to polarographs and other electrochemical instruments.[20] This topic is now included in several textbooks, and therefore will not be treated here in any detail. Over the years, the quality of these amplifiers has increased dramatically, and the cost has decreased almost as dramatically. At present, quite good solid-state amplifiers are available in small packages (dual in line, TO-99, etc.) at a cost of only a few dollars each. Naturally, these have resulted in improved instrument performance, at lower cost and in a smaller package. The size of the instrument is often dictated by the size of the control panel needed to accommodate all the switches and dials.

As operational amplifiers have become more commonly used in polarographic circuits, there has been a tendency in research articles to say less about the instrumentation, and often only a block diagram is given. However, Buchanan and McCarten[21] give considerable detail on their square-wave polarograph. Krause and Ramaley[22] give only a block diagram of their instrument, but Liddle[17] gives a quite detailed discussion of his instrument in his Ph.D. thesis. All three of these instruments use a potentiostat in which the control amplifier is operated with the noninverting input grounded, and the inverting input serves as the summing point for all signals. Only the instrument described by Liddle[17] employs a positive-feedback loop. Krause and Ramaley[22] as well as Liddle[17] use two gated sample and hold circuits to measure the current as the specified points on the two halves of the square-wave cycle.

The two sample and hold circuits serve as inputs to a final difference amplifier, which then outputs the processed current signal to an X-Y recorder. Buchanan and McCarten[21] gate the output of the current amplifier into a full-wave rectifier circuit and then to the recorder. All three of these instruments use digital circuits to generate the square-wave signal and the gate-control signals. The instrument of Krause and Ramaley[22] was used only with a stationary electrode; that of Buchanan and McCarten[21] used a D.M.E. with no regulation of drop time; Liddle's[17] instrument used a solenoid drop detacher, driven by the digital timing logic.

Liddle[17] discovered that the sample and hold units that he used (Philbrick SPT & H Modulators) were so fast that they tracked high-frequency noise during the sampling time and did little to filter it. Even after these units were modified to obtain some filtering action, they were not totally satisfactory. Based on this experience, Sturrock and Carter[19] decided to use a gated integrator between the current amplifier of the potentiostat and the two sample and hold circuits. Figure 5 is a functional diagram of their instrument, which was designed and constructed by Gerald O'Brien. In contrast to the instruments described above, the working electrode is hard-wired to the instrument ground, and the cell current is measured by the voltage drop across a resistor located between the output of the control amplifier and the counter electrode. This configuration results in greater stability of the potentiostat and eliminates the need for a current booster after the current amplifier. However, this configuration requires a high level of common-mode signal rejection in the current amplifier. The weak point in this instrument is the positive-feedback loop; which uses two inverting amplifiers. This results in too long a signal propagation delay, and the feedback signal is thus too far out of phase for proper operation. The final result is that the IR compensation is inadequate, and the cell-potentiostat rise time is not as fast as it should be. Even so, the detection limits of several metal ions are less than $1 \times 10^{-8} M$ with this instrument (see Figure 2), using a D.M.E. and a delay of 0.8 msec between potential step and the start of current integration.

The instrument was designed to operate with electrodes of 1 or 2 cm^2 area, such as a rotating-disk electrode, and the design was not optimized for use with a D.M.E. The original timing circuit allowed square-wave frequencies of 20, 50, 100, 200, 500, and 1,000 Hz. Later, a redesigned timing circuit was built, which featured synchronization with the 60-Hz line frequency so that all operations were repeated at the same time in the 60-Hz noise cycle. Two square-wave frequencies, 30 and 15 Hz, are available. Recently the instrument was modified to increase the delay before sampling to 1 msec and to facilitate digital data acquisitions by a laboratory computer. However, these modifications have not been evaluated yet.

Recently, O'Brien[23] suggested several modifications to the instrument of Sturrock and Carter. The first suggestion is to replace the two analog sample and hold circuits with an analog-to-digital converter and two digital registers. This would eliminate the drift problems associated with the sample and hold circuits and allow the accumulation of the difference currents over the life of one D.M.E. drop or whatever time unit is desired. A second suggestion is to improve the positive-feedback loop by replacing the two amplifiers with a voltage divider and a multiplying-type digital-to-analog converter. The digital inputs would be set by front panel switches to select the desired amount of positive feedback. The third suggestion is to utilize the first two sec of drop growth, during which the current is not sampled, to automatically zero the current amplifier, correct for the common-mode error signal of that amplifier, and correct for the drift in the analog integrator. This operation would make use of the analog-to-digital converter mentioned in the first suggestion.

Barker, Gardner and Williams[24] give a brief description of a new multimode polarograph, but unfortunately they give no details of the circuit. The instrument is designed to be capable of operation with a data processor.

The instrument constructed by Liddle[17] has now been modified for operation with a computer. The computer drives a digital-to-analog converter, which in turn supplies all potential excitation for the potentiostat. The computer also samples the current signal of the potentiostat, converts the analog signal to a digital representation, and does averaging and other processing on the data. Final output can be a computer printout or an X-Y plot. The instrument is quite flexible, as only program changes need to be made to perform a number of different polarographic techniques.

Ramaley[25] describes a new digitally controlled

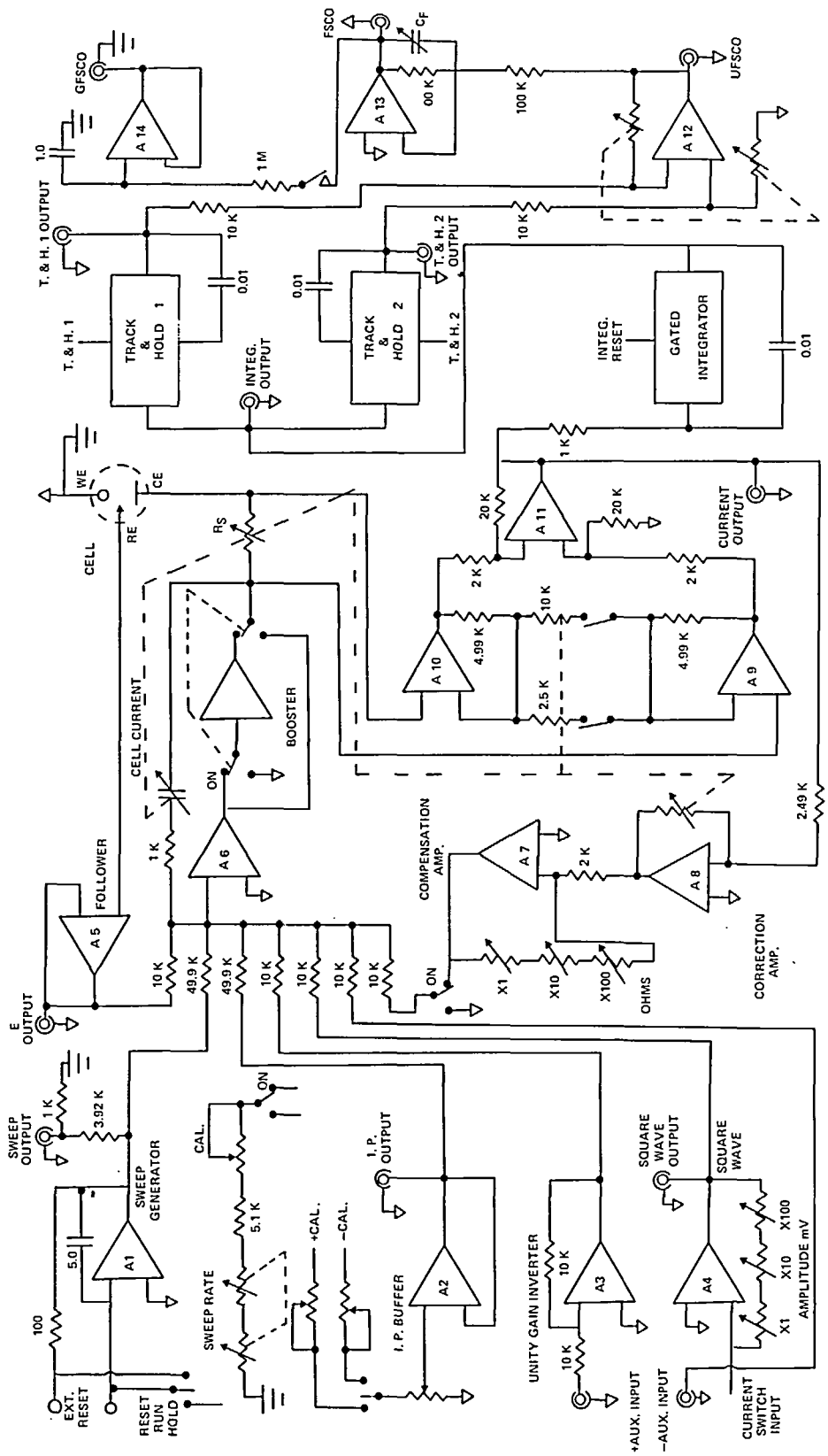

FIGURE 5. Square-wave polarograph functional diagram. All resistances are in ohms and capacitances are in microfarads. Abbreviations employed: GFSCO – gated, filtered, sampled cell current; UFSCO – unfiltered sampled cell current; INTEG. – integrator; AUX. – auxiliary; EXT. – external; I.P. – intial potential; WE – working electrode; CE – counter electrode, RE – reference electrode.

potentiostat for electrochemical studies and discusses its application for Tast polarography, staircase voltammetry, square-wave polarography, and square-wave voltammetry. The analog circuits of the potentiostat appear to be similar to that of his earlier instrument.[22]

Unfortunately, there seem to be no commercially manufactured square-wave polarographs of modern design. Such instruments will be necessary before square-wave polarography becomes widely used.

C. Pulse Polarographs

Developments in pulse polarographs have been similar to those in square-wave polarographs. However, the application of digital computers to pulse polarography predated the application to square-wave polarography, and several modern commercial instruments have been produced.

Parry and Osteryoung[26] made a preliminary report on a new instrument. They reported a determination of a species undergoing a two-electron transfer, at the $10^{-7}M$ level. The instrument could be operated in either the differential or normal mode. In a later paper,[15] the same authors give an evaluation of analytical pulse polarography using this instrument. The instrument used a pulse of 50-msec width and variable magnitude. The current was sampled prior to pulse application and after a delay of 40 msec. Unfortunately, the detailed description of this instrument was never published.

Lauer and Osteryoung[27] describe a general-purpose laboratory data acquisition and control system and describe its application to chronocoulometry and to pulse polarography.

Another instrument was reported by Keller and Osteryoung.[28] This instrument appears to be an updated version of that reported by Lauer and Osteryoung.[27] The analog circuitry of the instrument is simply described as being "conventional." Some specifications are given for the analog-to-digital and digital-to-analog converters. The instrument is claimed to give "useful data" for $4 \times 10^{-8}M$ Cd^{2+}, 10% precision for $4 \times 10^{-7}M$ Cd^{2+}, and is projected to have a limit detection below $1 \times 10^{-8}M$ Cd^{2+}.

These measurements were made on a hanging-mercury-drop electrode (H.M.D.E.). With this instrument, variations of pulse width, heights, sampling delay, and time between pulses are all possible. It is shown that polarograms obtained with shorter pulse widths (and therefore shorter delays before current sampling) had higher peak heights, as is theoretically predicted. However, no results were reported with sampling delays of less than 10 msec. It was also suggested that positive feedback would increase sensitivity. Another advantage of the instrument is the ability to do ensemble averaging and digital smoothing of the results.

Several commercial pulse polarographs were discussed by Burge.[29] It is interesting to note that the only commercial instruments that have a variable sampling delay are those based on Barker's design (Southern-Harwell Model A1700 and A1300) that use a two-electrode cell configuration. The delay before sampling can be varied from 2 to 40 msec. The other instruments use a three-electrode cell configuration, but have fixed delay times of 40 msec or greater. The Melab Model CPA-3 uses a 100 msec pulse width and samples for 33 1/3 msec after a 50-msec delay. The 33 1/3-msec sampling time was chosen to allow averaging over two 60-Hz noise cycles. The Princeton Applied Research Models 170 and 171 use a pulse width of 48 msec and average current for 8 msec after a delay of 40 msec.

The Melab instrument and the Southern-Harwell instruments can operate in either the differential-pulse mode or the normal-pulse mode. However, the P.A.R. instruments do not have the differential-pulse mode. Instead, they have the normal-pulse mode and also a derivative mode in which the differences between successive pulses are recorded. This results in a polarogram similar in appearance to that of the differential-pulse mode, but not as sensitive.

Subsequent to the article by Burge,[29] Princeton Applied Research introduced their Models 174 and 174A. These instruments do have a true differential-pulse mode and have come into common use because of their high quality and reasonable price. These instruments use a 16.7-msec sampling of the current before pulse application and a 40-msec delay before a second 16.7-msec sample is taken. The differences of the two currents are recorded. This is a type 2 instrument as defined by Christie and Osteryoung[14] (see Section III C).

As this paper was being written, Princeton Applied Research was preparing to introduce a new instrument. The instrument is reportedly based around a microprocessor. No further details

were available prior to formal introduction of the instrument.

V. APPLICATIONS

A. Non-stripping Techniques

1. Square-wave Polarography

The first applications of square-wave polarography were reported by Ferrett and coworkers.[7-10] However, applications have been limited by the lack of good commercial instrumentation at reasonable cost. Buchanan and Bacon[30] used square-wave polarography to monitor effluents of ion-exchange columns. They modified the instrument of Buchanan and McCarten[21] so that it sequentially sampled the current at the peak potentials of Cu^{2+}, Pb^{2+}, Cd^{2+}, and Zn^{2+}. Buchanan, Schroeder and Novosel[31] used square-wave polarography to survey the levels of Pb^{2+} in river water, and Novosel and Buchanan[32] also studied levels of Cu^{2+} in potable water and river water.

Yoshimur reported the simultaneous determination of copper, lead, and zinc in high-purity aluminum[33] and the determination of lead by coprecipitation with zirconium hydroxide.[34] Komatsu and Kakeyama[35] reported the determination of cyanide ions. Komatsu, Matsueda and Kakeyama[36] reported the determination of Cu^{2+}, Pb^{2+}, Cd^{2+}, and Zn^{2+} in water by square-wave anodic stripping.

Sturrock and Carter[19] studied the square-wave polarography of 13 metals. Each ion was studied in several supporting electrolytes to determine the experimental conditions for maximum sensitivity. Their results are summarized in Table 2. The lower

TABLE 2

Metal ion	Supporting electrolyte	E_s (vs SCE)	Remarks*
Sb (III)	1. 1F HCl	-0.15 V	(1) w (2) The major interferences are the mercury dissolution wave, Bi (III), and relatively high concentrations of Cu (II) (3) 7×10^{-8} F or 8.5 ppb
	2. 1F HNO_3	-0.30 V	NA
	3. 0.5F H_2SO_4-0.01F KCl	-0.21 V	(1) p (2) The poorly defined wave does not allow very low determinations (3) 4×10^{-7} F or 49 ppb
	4. 1F HNO_3-0.02F KCl	-0.17 V	(1) p (2) The peak is larger and better defined than 1F HNO_3 (3) 3×10^{-7} F or 37 ppb
	5. 0.5F H_2SO_4-0.05F HCl	-0.14 V	(1) fw (2) The mercury dissolution wave is not a considerable problem (3) 8×10^{-8} F or 9.7 ppb
	6. 0.24F sodium tartrate, pH 4.4 (adjusted with HCl)	NA	NA [a wave was not observed for 8×10^{-7} F Sb (III)]
	7. 0.5F HCl	-0.14 V	(1) w (2) The mercury dissolution wave is less of a problem than 1F HCl (3) 5×10^{-8} F or 6.1 ppb
AS (III)	1. 1F HCl	-0.44 V	(1) f (2) Pb (II), Sn (IV), and Tl (I) are interferences; however, the baseline is fairly flat (3) 8×10^{-8} F or 6.0 ppb

*(1) Reversibility: vp (very poor), p (poor), f (fair), fw (fairly well), w (well defined). (2) General comments. (3) Approximate detection limit [F and parts per billion (ppb)]. NA = not applicable.

TABLE 2 (continued)

Metal ion	Supporting electrolyte	E_s (vs SCE)	Remarks
	2. 0.5F H_2SO_4-0.5F HCl	−0.45 V	(1) vp (2) An ill-defined As (III) wave is obtained in this medium (3) 8×10^{-7} F or 60 ppb
	3. 1F HNO_3-0.02F KCl	NA	NA
	4. 0.1F H_2SO_4	−0.69 V	(1) vp (2) This electrolyte allows separation from common interferences (3) 8×10^{-7} F or 60 ppb
	5. 0.25F sodium tartrate, pH 4.4	NA	NA
	6. 0.5F HCl	−0.44 V	(1) f (2) The peak appears to be at least as sharp as in 1F HCl, and the impurity level is lower in 0.5F HCl (3) 5×10^{-8} F or 3.7 ppb
Bi (III)	1. 0.5F HCl	−0.06 V	(1) w (2) The mercury dissolution wave severely interferes if the acid concentration is increased to 1F; the summit potential in 1F HCl is −0.09 V, and the mercury dissolution interference is even more severe (3) 8×10^{-7} or 167 ppb
	2. 0.05F H_2SO_4	−0.04 V	NA
	3. 0.25F sodium tartrate, pH 4.4 (adjusted with HCl)	−0.24 V	(1) fw (2) This electrolyte allows a fairly effective separation of the copper and mercury dissolution interferences (3) 1×10^{-7} F or 21 ppb
Cd (II)	1. 0.1F KNO_3, pH 3.5	−0.58 V	(1) w (2) Excellent supporting electrolyte for simultaneous Pb (II), Cu (II), Zn (II), and Cd (II) analysis (3) 1×10^{-8} F or 1.1 ppb
	2. 0.1F Na_2SO_4, pH 3.5	−0.59 V	(1) w (2) Excellent supporting electrolyte for the determination of Cd (II) (3) 1×10^{-8} F or 1.1 ppb
	3. 0.1F KCl, pH 3.5	−0.60 V	(1) w (2) Chloride medium is excellent for the determination of Cd (II), Pb (II), Cu (II),and Zn (II) (3) 6×10^{-9} F or 0.7 ppb
	4. 0.1F KH_2PO_4, pH 4	−0.59 V	(1) w (2) This is an excellent supporting electrolyte because of its pH buffering
	5. 0.1F NH_4Cl-0.1F NH_4OH	−0.69 V	(1) w (2) An excellent supporting electrolyte with a buffered pH
	6. 0.1F $(NH_4)_2$ tartrate-0.1F NH_4OH	−0.73 V	(1) w (2) A fairly good medium for the determination of Cu (II), Fe (III), Pb (II), Cd (II), and Zn (II)
	7. 0.09F sodium acetate, pH 4.75 (adjusted with HNO_3)	−0.59 V	(1) w (2) An excellent supporting electrolyte with pH buffering (3) 1×10^{-8} F or 1.1 ppb
	8. 0.09F KNO_3 with 0.01F borax, pH 7.2	−0.58V	(1) w (2) The higher pH has no apparent affect on the reversibility of the Cd (II) wave

TABLE 2 (continued)

Metal ion	Supporting electrolyte	E_s (vs SCE)	Remarks
	9. 0.09F KNO_3 with 0.01F tartrate, pH 4	-0.58 V	(1) w (2) Probably the best supporting electrolyte found for the simultaneous determination of Pb, Cd, Cu, and Zn (3) 8×10^{-9} F or 0.9 ppb
Co (II)	1. 1F KSCN	-1.10 V	(1) p (2) The background is not very good for the determination of Co (II) and Ni (II) (3) 8×10^{-7} F or 47 ppb
	2. 0.1F KSCN	-1.10 V	(1) p (2) A little better background is observed with 0.1F KSN as compared to 1F KSCN (3) 8×10^{-7} F or 47 ppb
	3. 0.1F KNO_3 with 0.01F ethylene diamine	-0.47 V	(1) fw (2) The Ni (II) wave is not very well defined, and Pb (II) (E_s = -0.56 V) may interfere (3) 3×10^{-7} F or 18 ppb
	4. 0.1F NH_4Cl-0.1F NH_4OH	-1.18 V	(1) fw (2) The optimal electrolyte found for the simultaneous determination of Co (II), Ni (II), and Mn (II) (3) 2×10^{-7} F or 12 ppb
Cu (II)	1. 0.1F KNO_3, pH 3.5	+0.01 V	(1) w (2) Excellent for the determination of Cu (II) in the presence of Fe (III) (3) 2×10^{-8} F or 1.3 ppb
	2. 0.1F KH_2PO_4	-0.01 V	(1) w (2) The mercury dissolution wave limits the determination of submicroformal levels (3) 2×10^{-7} F or 13 ppb
	3. 0.1F KCl, pH 3.5	-0.15 V	(1) fw (2) The mercury dissolution wave limits the determination of Cu (II) (3) 8×10^{-8} F or 5.2 ppb
	4. 0.09F sodium acetate pH 4.75 (adjusted with HNO_3)	-0.01 V	(1) w (2) The mercury dissolution wave limits the determination of Cu (II)
	5. 0.1F KNO_3 with 0.01F borax, pH 7.2	-0.03 V	(1) fw (2) The reversibility of the copper wave is affected by the relatively high pH (3) 5×10^{-8} F or 3.2 ppb
	6. 0.1F NH_4Cl-0.1F NH_4OH	-0.15 V -0.38 V	(1) w (2) The first wave [Cu (II) → Cu (I)] is smothered by the mercury dissolution wave
	7. 0.1F $(NH_4)_2$ tartrate-0.1F NH_4OH	-0.15 V -0.38 V	(1) w (2) This electrolyte allows separation from relatively small concentrations of Fe (III) (3) 8×10^{-6} F or 5.2 ppb
	8. 0.1F $(NH_4)_2C_2O_4$-0.1F NH_4OH	-0.18 V -0.38 V	(1) w (2) This electrolyte allows effective separation from the Fe (III) → Fe (II) wave (3) 8×10^{-6} F
	9. 0.09F KNO_3 with 0.01F tartrate, pH 4		(1) w (2) This is an excellent supporting electrolyte for the simultaneous determination of Pb (II), Cu (II), Cd (II), and Zn (II) (3) 2×10^{-6} F or 1.3 ppb

TABLE 2 (continued)

Metal ion	Supporting electrolyte	E_s (vs SCE)	Remarks
	10. 0.1F KNO_3 with 10^{-3}F $K_2C_2O_4$, pH 4	−0.12 V	(1) w (2) 0.01F $K_2C_2O_4$ (pH4) provides better pH buffering (3) 8×10^{-9}F or 1 ppb
Fe (III)	1. 0.1 F sodium pyrophosphate, pH 3.7	NA	NA (no wave was observed for 1×10^{-6}F Fe (III) in this supporting electrolyte
	2. 0.5F sodium tartrate, pH 12	NA	NA
	3. 01F NH_3Cl-0.1F NH_4OH with 0.01F ascorbic acid	NA	NA
	4. 0.1F $(NH_4)_2$ tartrate-0.1F NH_4OH	−0.47 V −1.42 V	(1) fw (2) This electrolyte allows a somewhat effective separation between the copper and iron waves (3) 2×10^{-7}F or 11.2 ppb
	5. 0.1F $(NH_4)C_2O_4$-0.1F NH_4OH	−0.29 V −1.56 V	(1) fw (2) This electrolyte allows an effective separation between Fe (III) and Cu (II)
	6. 0.2F KNO_3 with 0.01F $K_2C_2O_4$, pH 4	−0.14 V	(1) fw (2) Probably the best electrolyte for the determination of Fe (III) if Cu (II) is absent (3) 1×10^{-7}F or 5.6 ppb
	7. 0.1F KNO_3-0.1F $K_2C_2O_4$, pH 4	−0.21 V	(1) fw (2) The copper wave overlaps the iron wave in this medium also
	8. 0.1F KNO_3-0.1F $K_2C_2O_4$ with 0.008F EDTA, pH 4	−0.18 V	(1) p (2) Neither copper nor iron is masked by the addition of EDTA at pH 4
Pb (II)	1. 0.1F KNO_3, pH 3.5	−0.39 V	(1) w (2) Excellent for the simultaneous determination of Cd (II), Cu (II), Zn (II), and Pb (II) (3) 1×10^{-8}F or 2.1 ppb
	2. 0.1F Na_2SO_4, pH 4	−0.40 V	(1) w (2) Even if milliformal acetate or tartrate medium is added, the lead peak is still relatively smaller than in most other electrolytes
	3. 0.1F KH_2PO_4, pH 4	−0.40 V	(1) w (2) The peak height for 4×10^{-7}F (Pb (II)) is about one half the peak height in 0.1F KNO_3
	4. 0.1F KNO_3 with 10^{-3}F sodium acetate, pH 6.6	−0.41 V	(1) fw (2) The reversibility of the Pb (II) wave is affected by the higher pH
	5. 1F NaOH	−0.76 V	(1) fw (2) The electrolyte allows separation between Pb (II) Tl (I)
	6. 0.09F KNO_3 with 0.01F sodium tartrate, pH 4	−0.41 V	(1) w (2) An excellent electrolyte for the determination of Cd (II), Cu (II), Pb (II), and Zn (II) (3) 8×10^{-9}F or 1.7 ppb
	7. 0.09F KNO_3 with 0.01F borax, pH 7.2	−0.42 V	(1) fw (2) The reversibility for the Pb (II) wave is definitely affected by the higher pH
	8. 0.09F sodium acetate, pH 4.75 (adjusted with HNO_3)	−0.41 V	(1) w (2) This electrolyte affords pH buffering (3) 1×10^{-8}F or 2.1 ppb

TABLE 2 (continued)

Metal ion	Supporting electrolyte	E_s (vs SCE)	Remarks
	9. 0.1F KNO_3-0.05F NaF, pH 3.0	-0.39 V	(1) w (2) Glassware cannot be used if this electrolyte is employed
	10. 0.1F KCl, pH 3.5	-0.40 V	(1) w (2) Chloride medium is probably the best for the determination of Pb (II); the peak height for Pb (II) increases as the chloride concentration is increased (3) 5×10^{-9} F or 1 ppb
Mn (II)	1. 0.1F KCl with 0.02F NH_4OH	-1.49 V	(1) fw (2) The pH must be above 7 in order to observe the Mn (II) wave (3) 5×10^{-7} F or 27 ppb
	2. 0.1F KSCN	-1.50 V	(1) f (2) This electrolyte is not recommended for the determination of Mn (II) (3) 2×10^{-6} F or 110 ppb
	3. 0.1F NH_4Cl-0.1F NH_4OH	-1.51 V	(1) fw (2) The optimum electrolyte found for Mn (II) (3) 8×10^{-8} F or 4.4 ppb
Ni (II)	1. 0.1F KSCN	-0.71 V	(1) fw (2) A 10^{-6} F Ni (II) solution in this medium appears as a shoulder on the background (3) 8×10^{-7} F or 47 ppb
	2. 1F KSCN	-0.17 V	(1) fw (2) The mercury dissolution wave does not allow the determination of submicroformal concentrations
	3. 0.1F KNO_3 with 0.01F ethylene diamine	-0.65 V	(1) p (2) A broad wave is obtained for Ni (II) in this medium (3) 1×10^{-6} F or 59 ppb
	4. 0.1F NH_4Cl-0.1F NH_4OH	-0.93 V	(1) fw (2) The reversibility of Ni (II) in this electrolyte is almost equal to that of Cd (II) or Pb (II) (3) 8×10^{-8} F or 4.7 ppb
Tl (I)	1. 0.5F HCl	-0.48 V	(1) w (2) This electrolyte is excellent for the determination of Tl (II) if As (III), Pb (II), or Sn (IV) impurities are not present
	2. 0.1F KCl	-0.46 V	(1) w (2) Relatively high concentrations of Pb (II) interfere (3) 5×10^{-4} F or 10 ppb
	3. 1F KCl with 0.008F sodium EDTA, pH 4	-0.47 V	(1) w (2) pH is too low to effectively mask the Pb (II) interference; however, if the pH is too high (>11.0), the reversibility of the Tl (I) wave is affected
	4. 0.09 KNO_3 with 0.01F tartrate, pH 4	-0.46 V	(1) w (2) Pb (II) interferes in the determination of Tl (I) in this medium
	5. 0.2F sodium acetate-0.1F KCl, pH 4.75	-0.46 V	(1) w (2) Lead interferes with the determination of Tl (I) in this electrolyte

TABLE 2 (continued)

Metal ion	Supporting electrolyte	E_s (vs SCE)	Remarks
	6. 0.2F sodium acetate-0.1F KCl, pH 4.75, with 0.005F EDTA added	-0.47 V	(1) w (2) Lead interference is masked by the addition of EDTA; Cu (II) can also be determined with the employment of this electrolyte (3) 5×10^{-8} F or 10 ppb
	7. 1F NaOH	-0.48 V	(1) w (2) The Pb (II) wave occurs at -0.76 V
Sn (IV)	1. 0.1F HCl	-0.42 V	(1) p (2) The peak height and reversibility of the wave is much improved if a higher concentration of HCl is employed (3) 3×10^{-7} F or 36 ppb
	2. 0.5F HCl	-0.44 V	(1) w (2) The interferences are Pb (II), Tl (I), and As (III) (3) 5×10^{-8} F or 6 ppb
	3. 1F HOAc-1F NH_4Ac	-0.60 V	(1) fw (2) This electrolyte allows the Sn (II) → Sn^0 reduction wave to be effectively separated from Tl (I), Pb (II), and As (III)
	4. 0.5F sodium citrate, pH 4.5	-0.13 V	(1) f (2) The mercury dissolution wave interfered with the determination of low levels of Sn (IV)
	5. 1F NH_4Cl-0.25F HCl	-0.46 V	(1) w (2) If As, Tl, or Pb ions are not present, this electrolyte is excellent (3) 4×10^{-8} F or 4.8 ppb
Zn (II)	1. 0.1F KNO_3, pH 3.5	-0.99 V	(1) fw (2) The only commonly occurring interference is Ni (II) (3) 2×10^{-8} F or 1.3 ppb
	2. 0.1F Na_2SO_4, pH 4	-1.00 V	(1) fw (2) Ni (II) may interfere (3) 2×10^{-8} F or 1.3 ppb
	3. 0.1F KH_2PO_4	-1.00 V	(1) fw (2) The pH is buffered when this electrolyte is employed (3) 2×10^{-8} F or 1.3 ppb
	4. 0.09F KNO_3 with 0.01F borax, pH 7.2	-1.00 V	(1) fw (2) The hydrogen wave does not interfere at pH 7.2 (3) 2×10^{-8} F or 1.3 ppb
	5. 0.1F KNO_3 with 0.05F NaF, pH 3	-0.99 V	(1) fw (2) Glassware should not be employed with this electrolyte; the hydrogen wave interferes also
	6. 0.1F KNO_3 with 10^{-3} F $K_2C_2O_4$, pH 4	-1.01 V	(1) f (2) If the oxalate concentration is increased to 0.01F, a zinc wave is not observable if the zinc concentration is less than 2×10^{-7} F (3) 1×10^{-7} F or 6.5 ppb
	7. 0.09F NaAc, pH 4.75 (adjusted with HNO_3)	-1.00 V	(1) fw (2) This is an excellent supporting electrolyte for determination of Zn (II) (3) 2×10^{-8} F or 1.3 ppb
	8. 0.01F KCl, pH 7	-1.00 V	(1) w (2) The peak height of Zn (II) decreases as the chloride concentration is increased (3) 1×10^{-8} F or 0.7 ppb

limit of detection was estimated by measuring the peak heights at low concentrations and extrapolating to where the ratio of the analytical signal to background noise was three to one. An estimate of the lower limit of detection is not given if it is felt that a reasonable approximation cannot be obtained. The expression "NA" in columns three and four of Table 2 means that no wave was observed at $1 \times 10^{-6} M$ or that the medium is not acceptable as compared to the other electrolytes listed. The symbol F stands for formal concentration.

Figure 2 shows a polarogram obtained with the instrument used by these authors.[19]

Sturrock and Carter[19] also reported that, when the D.M.E. was replaced with a hanging-mercury-drop electrode (H.M.D.E), limits of detection for Pb^{2+} and Cd^{2+} were $3 \times 10^{-9} M$ and $4 \times 10^{-9} M$ respectively, as compared to $5 \times 10^{-9} M$ and $8 \times 10^{-9} M$ with the D.M.E. The results on the H.M.D.E. were for the forward sweep (+ to -) and did not include anodic stripping. Their anodic-stripping experiments are discussed below. In addition to increased sensitivity, the H.M.D.E. required less damping in the current-processing circuits, and the potential could be swept at a faster rate. However, persistent problems were encountered with the Beckman hanging-drop electrode assembly, and the use of this device was discontinued; the assembly was replaced with the Beckman rotating-disk electrode, as described below.

The information summarized in Table 2 should be applicable to pulse polarography, although the limits of detection are functions of the specific instrument used and will not necessarily apply to other instruments.

2. Pulse Polarography

The literature on applications of pulse polarography is much more voluminous than that of square-wave polarography, especially since the introduction of the Princeton Applied Research Model 174.

Parry and Oldham[37] studied the electrochemistry of palladium (II) in ammonia and pyridine media. In this paper it is shown that, as the pulse magnitude is increased, the widths of the peaks for these irreversible processes do not increase appreciably until pulses of greater than 60 mV are used. However, the peak heights increase linearly until pulses of greater than 80 mV are used. Thus larger pulses would seem to be indicated for irreversible processes, than for reversible processes.

Myers and Osteryoung[38] discussed amperometric titrations using differential-pulse polarography. They were able to carry out an EDTA titration of $2 \times 10^{-7} M$ Cu^{2+}. Their results also illustrate the problems of adsorption of Cu^{2+} on the walls of the cell, which is a serious problem at these levels. These same authors[39] report the determination of As (III) on the parts-per-billion level by use of anodic stripping. This article also contains references to many other applications of pulse polarography.

An application of pulse polarography to analysis of air pollutants is reported by Garber and Wilson;[40] they were able to determine SO_2, free of interferences from sulfides and sulfate, at the $5 \times 10^{-7} M$ level with an accuracy of 25%. Brooks, de Silva and D'Arconte[41] demonstrated the potential for applications of pulse polarography to clinical chemistry; they reported the determination of trimethoprim in blood and urine samples. Demerie, Temmerman and Verbeck[42] used pulse polarography to determine gallium in high-purity arsenic; however, it was necessary to separate most of the arsenic from the gallium prior to the polarography determination.

B. Stripping Analysis

Square-wave and pulse polarography have been employed as the detection system in anodic-stripping analysis since the first reported work of Barker and co-workers[1-6,11] and of Sturm and Ressel.[43] The electrodes used for these experiments were various forms of the H.M.D.E. However, recent work [44-46] has clearly shown the superiority of the thin-film mercury electrode, which results from a much larger ratio of the surface area to volume of mercury.

One problem that has become evident with the thin-film mercury electrodes is the formation of intermetallic compounds. The case of Cu-Zn is especially well documented.[47] Copeland, Osteryoung and Skogerboe[48] make the interesting observation that the interference by copper, in the analysis for zinc, can be eliminated by adding gallium, which preferentially forms an intermetallic compound with copper.

A second problem common to anodic-stripping analysis is lack of reproducibility. This is especially noticeable for thin-film electrodes, where the

TABLE 3

Summary of Optimal Experimental Conditions (RDE)

I. Chemical parameters
   A. Mercury plating procedure
      1. Mercury (II) Concentration – 4×10^{-4}F
      2. Mercury plating time – overnight quiescently, then rotating for 10 min at 80 rps or for approximately 20 min at 50 rps
      3. Plating potential – –300 mV (vs. SCE); if copper is to be determined, any copper impurity in the plate must be stripped out before changing to the test solution
   B. Supporting electrolytes – 0.09F sodium acetate (pH 4.75) with HNO_3 and 0.09F KNO_3 with 0.01F sodium tartrate (pH 4)
   C. Deaeration time – at least 2 min with electrode rotation
II. Instrumental parameters
   A. Square-wave voltage – 50 mV
   B. Sweep rate – 50 mV/sec
   C. Frequency – 30 Hz
   D. Positive feedback – adjusted for each scan
   E. Electrode rotation rate – 50 rps

manner of plating, thickness of mercury plate, etc., can have pronounced effects on the resulting peaks.

Sturrock and Carter[19] studied the application of square-wave polarography for anodic stripping from a mercury-film rotating-disk electrode. The electrode was rotated at 50 rps while plating, but the subsequent stripping was done on the stationary electrode. Like previous workers,[45] they obtained excellent results using the Beckman rotating-disk electrode fitted with a vitreous carbon tip. Unlike the previous workers, they found that the sensitivity continued to increase as the sweep rate for stripping increased, up to the limit of their instrument sweep rate, 50 mV/sec.

Table 3 contains a summary of the optimal conditions found by Sturrock and Carter.[19] They found that, for very low concentrations, a significant increase in peak heights was observed between the first and second scans on a new solution. However, only a small increase occurred for the next several scans, and repeated scans thereafter gave virtually identical peak heights. This effect is probably due to the formation of mercuric oxide on the electrode surface when a new solution containing oxygen was added to the cell. Several reducing agents, such as ascorbic acid and hydrazine, were added to the solution to reduce the oxygen, but their use did not produce any significant improvement. Mercury(II) ions ranging in concentration from $10^{-7}M$ to $10^{-3}M$ were added to the solution to be analyzed in order to obtain a fresh surface. The addition of high concentrations of mercury yielded spurious results, because the amount of mercury on the electrode surface was appreciably changed. The higher concentrations of mercury greatly affected the amount of plated mercury on the electrode surface. Extremely dilute mercury (II) concentrations (such as $10^{-7}M$) did not appreciably change the amount of mercury on the surface, but the effect of the oxide-formation problem was lessened.

The procedure finally adopted for running successive solutions was as follows. A new sample solution was introduced to the cell and deoxygenated for two to five min, with the electrode rotating and the potential at –1 V. The solution was not vigorously deaerated, because the impingement of nitrogen bubbles on the surface of the electrode resulted in the loss of mercury. After sufficient deaeration, the nitrogen stream was diverted in order to purge the cell above the solution. The potential was then scanned anodically to a potential of approximately –0. 1 V, where the potential was held for approximately 1 min to insure complete stripping out of lead and cadmium. Then the potential was reset to –1 V, the electrode rotated, and the metals of interest were plated for 1 to 5 min. The rotating electrode was then stopped, positive feedback was adjusted, and after a predetermined time delay (usually 30 sec after the electrode had been stopped) the anodic-stripping voltammogram was recorded.

Standard additions were usually made to the solution at this point, and since very small volumes were added (approximately 5 μl), deaeration was not necessary. The change in "sensitivity" (i.e., current measured for a given concentration) of the electrode when solutions were changed was not of vital concern, since calibration techniques were not employed. However, a significant change from one scan to another is of vital concern, since this invalidates the method of standard addition. The initial deaeration and plating step serves as a test run. The compensation, recorder sensitivity, etc., can be adjusted using the results of this run. The same procedure was employed for the analysis of the "spiked" solutions, and from the increases in peak heights the concentration of the initial solution was determined.

Inconsistent results were obtained when the

TABLE 4

The Results for the Analysis of EPA Water Standards Employing the Mercury Film RDE

Analysis number	Metal ion	Reagent blank (in ppb)	Reported concentration (in ppb)	Concentration found (in ppb)
1	Pb (II)	1.2	28.0	27.5
2	Cd (II)	0.2	1.8	1.7
3	Pb (II)	0.7	28.0	27.1
4	Cd (II)	1.2	1.8	1.0
5	Pb (II)	1.4	22.4	21.0
6	Cd (II)	1.2	1.4	1.0
7	Pb (II)	2.8	28.0	27.1
8	Cd (II)	0.2	1.8	1.4
9	Pb (II)	1.9	9.2	11.5
10	Cd (II)	1.6	1.6	1.5
11	Pb (II)	2.2	9.2	9.8
12	Cd (II)	1.1	1.6	1.6

solution was deaerated while the metals were being plated, because the convection is difficult to reproduce. If the electrode was rotated for approximately 1 min while at a potential of about -0.1 V, the peaks in successive voltammograms became significantly larger. However, if rotation was not employed at these potentials, very reproducible results were obtained.

If the electrode was allowed to be in contact with the solution for several days, wetting of the graphite material resulted. Usually each electrode tip was plated overnight, then rotated before use. At the end of the day, mercury was removed with dampened paper towels, and the bare electrode tip was stored dry. Another electrode tip was plated overnight.

A linear relationship was obtained when peak height versus concentration was plotted for solutions of lead and cadmium ranging in concentration from $10^{-9}M$ to $10^{-7}M$, employing a 5-min plating time. Above $10^{-7}M$, there is some curvature in the plot. To achieve linearity for higher concentrations, shorter plating times can be employed or the rotation rate can be decreased. Since the reduction of analysis time was one of the objectives of the study, plating time was usually decreased. The total analysis time, including deaeration, the test run, and the voltammogram of the unknown solution and the spiked solution, was less than 15 min.

The results obtained for the analysis of solutions prepared by dilution of EPA standard solutions, employing the optimal experimental conditions listed in Table 3 are given in Table 4. Probably the largest source of error in the results (Table 4) was the use of small micropipets (1–10 μl) for standard additions.

VI. SUMMARY

The theoretical and practical aspects of square-wave polarography and related techniques have been reviewed. From theoretical consideration, the sensitivity of these techniques depends upon the rise time of the cell-potentiostat combination. If this rise time is sufficiently fast, the sensitivity is limited by the DC capacitance current when using the D.M.E. When the H.M.D.E. is used, the sensitivity is limited by the pulse capacitance current or by electronic noise.

The sensitivity of square-wave polarography and pulse polarography are similar. It appears that the square-wave technique is slightly more sensitive, except for completely irreversible processes, where the pulse technique is clearly superior.

The sensitivity of these techniques is such that determination can be performed on most real samples without a time-consuming extraction or concentration step. A serious drawback of the techniques is the slowness of the sweep rates required with the D.M.E. (often 1 mV/sec).

Either the detection limit or the time for analysis can be improved for those metals that form mercury amalgams, by use of the thin-film mercury-plated rotating-disk electrode.

REFERENCES

1. Barker, G. C. and Jenkins, I., *Analyst,* 77, 685 (1952).
2. Barker, G. C. and Jenkins, I., A.E.R.E., C/R 924 (1956).
3. Barker, G. C. and Cockbaine, D. R., A.E.R.E., C/R 1404 (1957).
4. Barker, G. C., A.E.R.E., C/R 1563 (1957).
5. Barker, G. C., Faircloth, R. L., and Gardner, A. W., A.E.R.E., C/R 1786 (1958).
6. Barker, G. C., *Anal. Chim. Acta.,* 18, 118 (1958).
7. Ferrett, D. J. and Milner, G. W. C., *Analyst,* 80, 132 (1955).
8. Ferrett, D. J. and Milner, G. W. C., *Analyst,* 81, 193 (1956).
9. Ferrett, D. J., Milner, G. W. C., Shalgosky, S., and Slee, L. J., *Analyst,* 81, 506 (1956).
10. Ferrett, D. J., Milner, G. W. C., and Samales, A. A., *Analyst,* 79, 73 (1954).
11. Barker, G. C. and Gardner, A. W., *Z. Anal. Chem.,* 179, 79 (1960).
12. Sturm, F. V. and Ressel, M., *Microchem. J.,* 5, 53 (1961).
13. Ramaley, L. and Krause, M. S., Jr., *Anal. Chem.,* 41, 1362 (1969).
14. Christie, J. H. and Osteryoung, R. A., *Electroanal. Chem.,* 49, 30 (1974).
15. Parry, E. P. and Osteryoung, R. A., *Anal. Chem.,* 37, 1634 (1965).
16. Buchanan, E. B., Jr., private communication.
17. Liddle, J. A., Ph.D. thesis, Georgia Institute of Technology, Atlanta (1972).
18. Grahame, D. C., *J. Am. Chem. Soc.,* 71, 2975 (1949).
19a. Sturrock, P. E. and Carter, R. J., The Trace Analyses of Water for Selected Metallic Elements Employing Square-wave Polarography, ERCR 0874, Georgia Institute of Technology, Atlanta (1974).
19b. Sturrock, P. E. and Hayman, A., unpublished work.
20a. Brown, E. R. and Smith, D. E., *Anal. Chem.,* 40, 1411, 1968.
20b. Brown, E. R., Hung, H. L., McCord, T. G., and Smith, D. E., *Anal. Chem.,* 40, 1424, 1968.
21. Buchanan, E. B., Jr. and McCarten, J. B., *Anal. Chem.,* 37, 29 (1965).
22. Krause, M. S. and Ramaley, L., *Anal. Chem.,* 41, 1365 (1969).
23. O'Brien, G. E., private communication.
24. Barker, G. C., Gardner, A. W., and Williams, M. J., *Electroanal. Chem.,* 42, App. 21 (1973).
25. Ramaley, L., *Chem. Instrum.,* in press.
26. Parry, E. P. and Osteryoung, R. A., *Anal. Chem.,* 36, 1366 (1964).
27. Lauer, G. and Osteryoung, R. A., *Anal. Chem.,* 40, 30A (1968).
28. Keller, H. E. and Osteryoung, R. A., *Anal. Chem.,* 43, 342 (1971).
29. Burge, D. E., *J. Chem. Educ.,* 47, A81 (1970).
30. Buchanan, E. B. and Bacon, J. R., *Anal. Chem.,* 39, 615 (1967).
31. Buchanan, E. B., Jr., Schroeder, T. D., and Novosel, B., *Anal. Chem.,* 42, 370 (1972)
32. Novosel, B. and Buchanan, E. B., Jr., *Z. Anal. Chem.,* 262, 100 (1972).
33. Yoshimur, W., *Jap. Anal.,* 21, 475 (1972).
34. Yoshimur, W., *Jap. Anal.,* 21, 1346 (1972).
35. Komatsu, M. and Kakeyama, H., *Jap. Anal.,* 21, 315 (1972).
36. Komatsu, M., Makueda, T., Kakeyama, H., *Jap. Anal.,* 20, 987 (1971).
37. Parry, E. P. and Oldham, K. B., *Anal. Chem.,* 40, 1031 (1968).
38. Meyers, D. J. and Osteryoung, J., *Anal. Chem.,* 46, 356 (1974).
39. Meyers, D. J. and Osteryoung, J., *Anal. Chem.,* 45, 267 (1973).
40. Garber, R. W. and Wilson, C. E., *Anal. Chem.,* 44, 1357 (1972).
41. Brooks, M. A., de Silva, J. A. F., and D'Arconte, L. M., *Anal. Chem.,* 45, 263 (1973).
42. Demerie, W., Temmerman, E., and Verbeck, F., *Anal. Lett.,* 4, 247 (1971).
43. Sturm, F. V. and Ressel, M., *Z. Anal. Chem.,* 186, 63 (1962).
44. Copeland, T. R., Christie, J. H., Osteryoung, R. A., and Skogerboe, R. K., *Anal. Chem.,* 45, 995 (1973).
45. Copeland, T. R., Christie, J. H., Osteryoung, R. A., and Skogerboe, R. K., *Anal. Chem.,* 45, 2171 (1973).
46. Osteryoung, R. A. and Christie, J. H., *Anal. Chem.,* 46, 351 (1974).
47. Rogers, R. S., Ph.D. thesis, Clarkson College of Technology, Potsdam, N.Y. (1970).
48. Copeland, T. R., Osteryoung, R. A., and Skogerboe, R. K., *Anal. Chem.,* 46, 2093 (1974).